

BOSTON UNIVERSITY  
COLLEGE OF ENGINEERING

Thesis

**IMPROVED BRAINSTEM MODELING TO  
CHARACTERIZE THE EFFECT OF LOW  
SPONTANEOUS RATE FIBER LOSS ON AUDITORY  
NEUROPATHY**

by

**GRAHAM VOYSEY**

B.S., Boston University, 2006

Submitted in partial fulfillment of the  
requirements for the degree of  
Master of Science

2016

DRAFT

© 2016 by  
GRAHAM VOYSEY  
All rights reserved

Approved by

First Reader

---

H. Steven Colburn, PhD  
Professor of Biomedical Engineering

Second Reader

---

Barbara Shinn-Cunningham, PhD  
Professor of Biomedical Engineering

Third Reader

---

Allyn E. Hubbard, PhD  
Professor of Electrical and Computer Engineering  
Professor of Biomedical Engineering

DRAFT

We've heard a lot of models...and heard suggested that we should take things out of our models to figure out what's important. But in some sense, when I look at the diversity of models that have been presented so far—each of us leave *out* things. So maybe in some sense we've got a start towards that approach.

So I can ask this question two ways, but let me ask it this way: *What should we leave in?* What's the bare minimum we should leave in as we try to understand what's important about the function of the cochlea?

*David C. Mountain*  
*Mechanics of Hearing (Attica, Greece 2014)*

## Acknowledgments

DRAFT

# IMPROVED BRAINSTEM MODELING TO CHARACTERIZE THE EFFECT OF LOW SPONTANEOUS RATE FIBER LOSS ON AUDITORY NEUROPATHY

GRAHAM VOYSEY

## ABSTRACT

Hidden Hearing Loss (HHL) is an emerging topic of hearing research that focuses on peripheral pathologies which leave audiometric thresholds unchanged but significantly impair threshold-independent hearing performance. Primary among the proposed mechanisms of HHL is selective damage of low spontaneous rate (low SR) fibers of the auditory nerve (AN), yet no noninvasive quantitative measure of this mechanism yet exists in humans.

This work aimed to support the hypothesis that measuring changes in latency of Wave V of the Auditory Brainstem Response (ABR) can predict the magnitude of preferentially damaged contributions by low spontaneous rate fibers to the output of the auditory nerve. While the relationship between Wave V latencies and a psychophysical measure of HHL has been recently established, current biophysical models do not fully account for the observed results.

We hypothesize that this modeling deficit is largely a consequence of the deficiencies of current brainstem and midbrain models, particularly those of the Inferior Colliculus (IC) and Lateral Lemniscus (LL), where Wave V is thought to originate. To rectify those deficiencies, more sophisticated models of the midbrain and brainstem were incorporated. Nonlinear weighting of the auditory nerve response, as supported

by recent anatomical work, was also incorporated. To quantify the effects of these changes on modeling predictions, a comprehensive modeling tool was developed which allows parametric exploration of modeling space and direct comparison between major models of the auditory nerve and brainstem.

DRAFT

# Contents

<b>1</b>	<b>Introduction</b>	<b>1</b>
1.1	Motivation . . . . .	1
1.2	Implication of the auditory periphery in cochlear synaptopathy . . . .	1
1.3	Human psychophysical tests suggest a diagnostic measure . . . . .	2
1.4	Computational models of the periphery are not predictive . . . . .	3
<b>2</b>	<b>Literature Review</b>	<b>4</b>
2.1	Chapter Summary . . . . .	4
2.2	Cochlear Synaptopathy . . . . .	5
2.3	Physiology of the Auditory Nerve . . . . .	5
2.3.1	Spontaneous Rates of Fibers . . . . .	5
2.3.2	Low Spontaneous Rate Fibers Suffer Selective Losses . . . . .	5
2.3.3	Current Controversies . . . . .	5
2.4	Relevant Functional Neuroanatomy of the Auditory Midbrain . . . . .	5
2.4.1	The Dorsal Cochlear Nucleus . . . . .	5
2.4.2	The Ventral Cochlear Nucleus . . . . .	5
2.4.3	The Inferior Colliculus . . . . .	5
2.5	Auditory Modeling Environments . . . . .	5
2.5.1	The Carney Models . . . . .	5
2.5.2	The Verhulst Model . . . . .	5
2.6	Objective Measures of Cochlear Synaptopathy . . . . .	5
<b>3</b>	<b>Aims</b>	<b>6</b>



3.1	Aim I. Simulate the ABR response to a forward-masking task with variable SR contributions. . . . .	6
3.2	Aim II. Integrate improved brainstem models. . . . .	7
3.3	Aim III. Relate model responses to psychophysical measures. . . . .	8
<b>4</b>	<b>Methods</b>	<b>9</b>
4.1	Chapter Summary . . . . .	9
4.2	Overview of Modeling Framework . . . . .	9
4.2.1	Configuration options define a parameter space . . . . .	10
4.2.2	Model Parameters . . . . .	10
4.3	Peripheral Models . . . . .	12
4.3.1	The Verhulst Model . . . . .	12
4.3.2	The Zilany Model . . . . .	13
4.3.3	Variations in spontaneous rates between models . . . . .	13
4.3.4	Peripheral Model Output . . . . .	14
4.4	Auditory Nerve Response Models . . . . .	15
4.4.1	Modeling Contributions of Inner Hair Cells . . . . .	15
4.4.2	Weighting of IHC contribution . . . . .	15
4.4.3	Weighting of Fiber Types per IHC . . . . .	16
4.4.4	Modeling Synaptopathy . . . . .	18
4.5	Brainstem Models . . . . .	18
4.5.1	The Nelson Carney 2004 Brainstem . . . . .	19
4.5.2	The Carney 2015 Brainstem . . . . .	19
4.6	Stimulus Generation . . . . .	19
4.7	Automated Parameter Exploration . . . . .	20
4.7.1	Design of new experiments . . . . .	20
<b>5</b>	<b>Results</b>	<b>23</b>

5.1	Chapter Summary . . . . .	23
5.2	Tone in noise . . . . .	23
5.3	Effect of peripheral model . . . . .	24
5.4	Effect of Synaptopathy . . . . .	24
5.5	Effect of CF weighting . . . . .	24
5.6	Effect of brainstem model . . . . .	24
<b>6</b>	<b>Discussion</b>	<b>25</b>
6.1	Chapter Summary . . . . .	25
6.2	Verhulst Model developments . . . . .	25
6.3	Consequences of percentage weighting degradation for synaptopathy .	25
<b>7</b>	<b>Conclusion</b>	<b>26</b>
7.1	Chapter Summary . . . . .	26
	<b>References</b>	<b>27</b>

## List of Figures

4.1	Overview of the Corti modeling environment. . . . .	11
4.2	Variation in Spontaneous Rate as a function of frequency . . . . .	17
4.3	Cochlear Synaptopathy parameters . . . . .	19
4.4	Automated exploration of model parameters . . . . .	21

DRAFT

## List of Abbreviations

AN	.....	Auditory Nerve
ANR *	Auditory Nerve Response	
CN	.....	Cochlear Nucleus
CS	.....	Cochlear Synaptopathy
HHL	.....	Hidden Hearing Loss
IC	.....	Inferior Colliculus
IFR	.....	Instantaneous Firing Rate
SR	.....	Spontaneous Rate

# Chapter 1

## Introduction

### 1.1 Motivation

The variability of overall performance between normal hearing listeners, particularly in super-threshold tasks performed in complex acoustic environments such as the cocktail party problem, has been recognized in the literature for many years. Until recently, this variability was largely attributed to a broadly-defined “Central Processing Disorder” in the absence of Noise-Induced Hearing Loss (NIHL). The performance of the auditory periphery has been thought to be sufficiently characterized by audiometric threshold testing, as well as Distortion-Product Otoacoustic Emissions (DPOAEs) and ABR for finer-grained assessments of peripheral function.

### 1.2 Implication of the auditory periphery in cochlear synaptopathy

Recently, selective deafferentation of low spontaneous rate fibers of the AN in the auditory periphery that do not affect audiometric thresholds have been convincingly demonstrated in mouse (Kujawa and Liberman, 2009), gerbil (Furman et al., 2013), and recently, chinchilla (Liberman, unpublished); a growing body of psychophysical evidence suggests that a similar pathology occurs in humans (Bharadwaj et al., 2015). Synaptic damage at the hair cell in the Organ of Corti has been observed both in

response to noise with intensities sufficient to induce a temporary threshold shift (TTS), which does not permanently affect thresholds or hair cell life, and due to age alone in quiet (Sergeyenko et al., 2013; Fernandez et al., 2015). This phenomenon has been variously described as “cochlear synaptopathy” (Bharadwaj et al., 2014), “auditory neuropathy”, or “Hidden Hearing Loss”.

It is now thought that selective low-SR loss is a hallmark of HHL. Consequently, it has been implicated in performance degradation in cocktail party scenarios in normal-hearing listeners (Bharadwaj et al., 2015, 2014). Unlike NIHL, no objective and noninvasive measure of HHL in humans has been established. While work is ongoing in cadaveric studies, the relationship between low-SR damage and HHL in humans has relied on inference from a combination of ABR, DPOAE, and psychometric measures, and no direct measure has yet been demonstrated that specifically implicates low-SR fiber loss as a causative factor.

### **1.3 Human psychophysical tests suggest a diagnostic measure**

Towards this goal of defining an objective measure of fiber loss, Mehraei et al. (2015, 2016) have performed a series of experiments that relate psychophysical performance in a tone in noise detection task to measured latency changes in ABR wave V as a function of signal to noise ratio. They hypothesized that the loss of low-SR/high-threshold AN fibers would contribute to a faster recovery time of the compound action potential of the AN. In a perceptual task, this translates to higher thresholds, and faster threshold recovery. In a group of 28 NHT subjects, comparison of ABR data and psychoacoustic performance demonstrate a relationship consistent with an impairment in low-SR population response.

## **1.4 Computational models of the periphery are not predictive**

While psychophysical experiments have supported the hypothesis of the importance of low-SR fibers, modeling the response of the auditory periphery, brainstem, and midbrain to the stimuli used in experiments has so far failed to produce results that align with experiment or intuition.

This thesis seeks to investigate the causes of this disparity, and proposes several novel additions to two auditory models to remedy it.

DRAFT

## Chapter 2

# Literature Review

### 2.1 Chapter Summary

This chapter lays out a review of the relevant literature this thesis relies on. First, an overview of the clinical significance and relevant neuroanatomy of cochlear synaptopathy are given. Then, a review of the computational models that will be used is presented.



## 2.2 Cochlear Synaptopathy

## 2.3 Physiology of the Auditory Nerve

### 2.3.1 Spontaneous Rates of Fibers

### 2.3.2 Low Spontaneous Rate Fibers Suffer Selective Losses

### 2.3.3 Current Controversies

## 2.4 Relevant Functional Neuroanatomy of the Auditory Mid-brain

### 2.4.1 The Dorsal Cochlear Nucleus

#### The Small Cap Area

### 2.4.2 The Ventral Cochlear Nucleus

### 2.4.3 The Inferior Colliculus

## 2.5 Auditory Modeling Environments

### 2.5.1 The Carney Models

#### The Zilany and Bruce Models

#### Modulation Transfer Functions in the Inferior Colliculus

### 2.5.2 The Verhulst Model

## 2.6 Objective Measures of Cochlear Synaptopathy

## Chapter 3

### Aims

This thesis investigates the models of the peripheral and central auditory systems and the utility of their predictive abilities of cochlear synaptopathy.

Three aims were established. First, to develop a coherent modeling environment that combines two leading models of the auditory periphery into one software package where the utility of each model could be compared head to head. Second, to advance the state of the models of the auditory periphery by extending them with new capabilities supported by available anatomical and physiological research. Third, to use the developed tool to explore the proposed mechanisms underlying psychophysical and large-scale electrophysiological studies of cochlear synaptopathy with higher fidelity.

#### **3.1 Aim I. Simulate the ABR response to a forward-masking task with variable SR contributions.**

A modeling environment was created. It incorporates two peripheral models of the auditory system: the Zilany model with humanized parameters (Zilany et al., 2014) and the Verhulst model (Verhulst et al., 2015).

The Cochlea modeling environment (Rudnicki and Hemmert, 2014) was used to provide easy integration of the Zilany model. The transmission-line model of Verhulst et al. (2015), which has the potential to perform better in broadband noise and ac-

counts for cochlear dispersion, was directly integrated. At the conclusion of this aim, direct comparisons between the outputs of Zilany et al. (2014) and Verhulst et al. (2015) were performed.

### **3.2 Aim II. Integrate improved brainstem models.**

We hypothesized that the current approach to IC modeling taken in Verhulst et al. (2015); Mehraei et al. (2016) does not fully account for the responses to a low-SR knockout AN model, and consequently under-represents the effects on the ABR wave V that have been experimentally measured.

In particular, an extension of the approach currently taken by Verhulst et al. (2015) was presented by Carney et al. (2015). It provides multiple classes of IC neurons that were shown to track complex tones (vowel formants) in noise. To guide the selection of model weights and connectivities, relevant neuro-anatomical literature were consulted. Crucially, studies by Ryugo (2008) and others have shown selectivities in SR projections to the small cap of the DCN, which will guide modeling work by introducing specificities in weighting. Further, while the latency change trend is preserved between both the models proposed by Zilany et al. and Verhulst et al., the magnitude of the effect is greatly different.

This discrepancy may be remedied by introduction of new IC modeling components, which are better incorporated in the Zilany et al. (2014) model.

### **3.3 Aim III. Relate model responses to psychophysical measures.**

We will compare subject Wave V latency data from Mehraei and Mehraei et al. as ground truth to the improved model output.

DRAFT

## Chapter 4

# Methods

### 4.1 Chapter Summary

This chapter gives a detailed description of the modeling environment created for this thesis. First, the configuration of the overall system is detailed. Second, the configuration and use of two models of the auditory periphery are detailed. Third, the creation of compound action potentials and population responses of the auditory nerve are given. A method for the simulation of cochlear synaptopathy is also detailed, along with a new incorporation of a nonlinear distribution of auditory nerve fiber types as a function of center frequency. Fourth, the use of these auditory nerve responses in simulation of the auditory brainstem and midbrain with two models are given, culminating in the creation of modeled Auditory Brainstem Responses. Finally, the utility of the system for large-scale simulation is shown.

### 4.2 Overview of Modeling Framework

The modeling framework created for this thesis has been named Corti(Voysey, 2016). It is architecturally inspired by the EarLab project developed at Boston University as well as the Cochlea(Rudnicki and Hemmert, 2014) modeling environment developed at the Technical University of Munich, from which it incorporates a peripheral model.

Corti is a command-line tool written in Python. As detailed in Figure 4-1, it is designed to produce estimates of the Auditory Brainstem Response, auditory nerve fiber, auditory nerve, brainstem and midbrain responses to an arbitrary stimulus. A set of configuration parameters define which models are used and how they are interconnected, as well as the spatiotemporal properties of the stimulus.

#### **4.2.1 Configuration options define a parameter space**

As detailed in Chapter 2, the constituent models of this framework each require many choices of parameters, ranging from sampling frequency to the time constants and relative inhibitory and excitatory contributions of brainstem areas. Several other parameters are introduced in the framework itself, as well as the choice of which model to use for each stage. Because these parameter choices directly modulate the simulation output, it quickly becomes natural to treat these different options as a high-dimensional parameter space. Any single run of the framework, using one collection of options, defines a particular trajectory through this space.

#### **4.2.2 Model Parameters**

To run a simulation, the following parameters must be given. Each parameter will be detailed in subsequent sections of this chapter.

1. The periphery model type.
2. Which components of the peripheral response to save to disk for later analysis.
3. The degree and kind of cochlear synaptopathy to simulate.
4. Whether or not the distribution of fibers per inner hair cell should vary as a function of basilar membrane location.

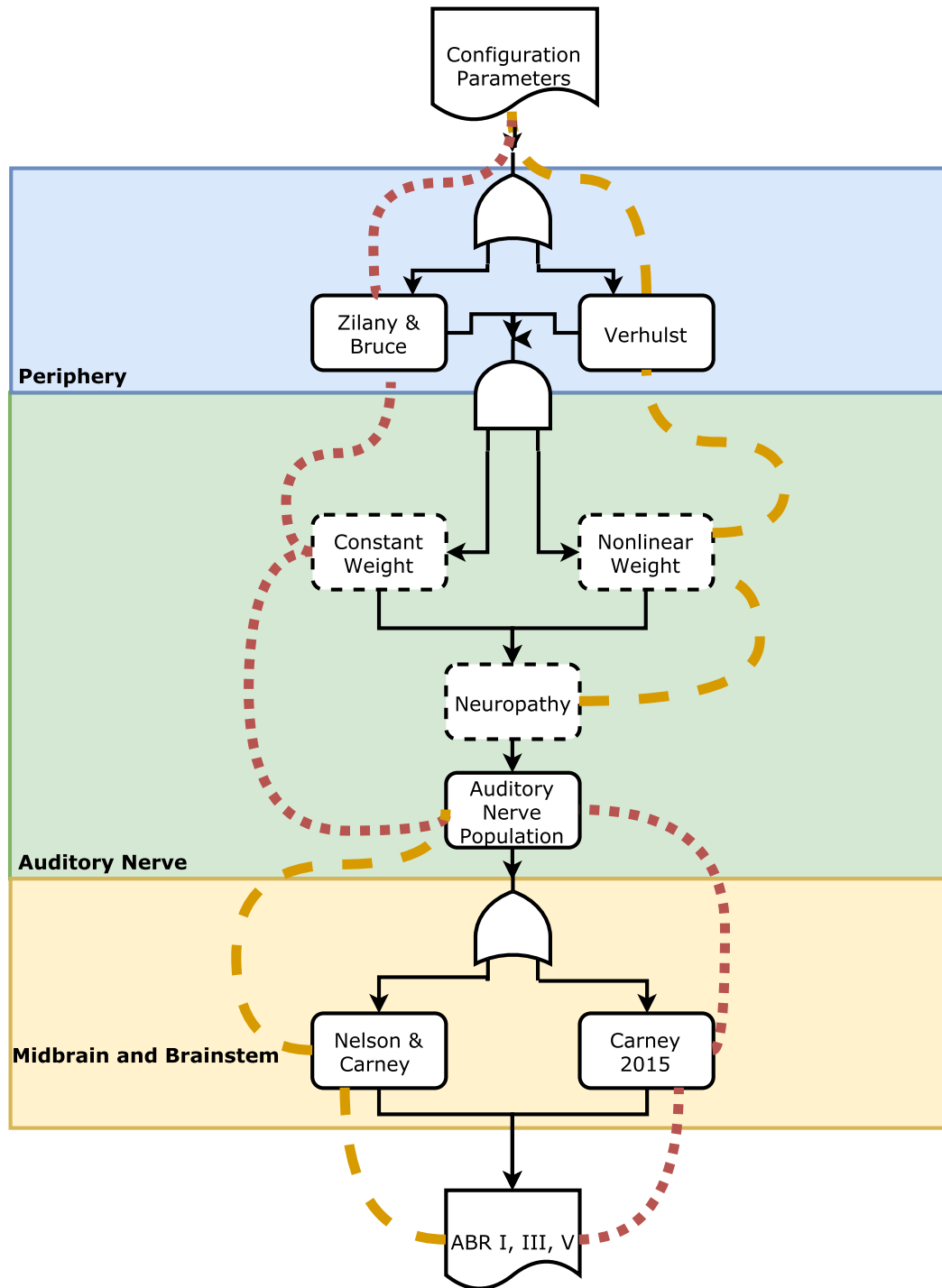


**Figure 4-1: Overview of the Corti modeling environment.** Two parameter trajectories are shown: a simulation of auditory neuropathy using the Verhulst periphery, nonlinear weights of fiber type contributions, and the Nelson and Carney brainstem (orange), and a simulation without neuropathy using the Zilany periphery, linear fiber weighting, and the Carney 2015 brainstem (red).

5. Whether or not a brainstem/midbrain response should be simulated.
6. The brainstem/midbrain model type.
7. The stimulus to simulate a response to.
8. The stimulus level.
9. Whether or not the model is being run as part of a larger parallel simulation.

### 4.3 Peripheral Models

Two models of the auditory periphery are included: the transmission-line model by Verhulst et al. (2015) (henceforth “The Verhulst model”) and the phenomenological model by Zilany et al. (2014) (henceforth “The Zilany model”). This section corresponds to the first stage of Figure 4-1, highlighted in blue.

Both models simulate the response of the peripheral auditory system to a pressure wave, and both produce timeseries estimates of instantaneous firing rates for an arbitrary number of inner hair cells which are tonotopically distributed along the length of the basilar membrane.

#### 4.3.1 The Verhulst Model

The Verhulst model is particularly well-suited for modeling broadband stimuli. Since it is a transmission line model which gives estimates for the position and deflection of the entire basilar membrane even to a pure tone stimulus, it naturally accounts for dispersive effects, and produces detailed information about many stages of sound propagation. Though not used in this work, the Verhulst model is also capable of modeling otoacoustic emissions in response to complex stimuli.



Since the development of the Verhulst model is still underway, it has been programmatically isolated in a separate package. This provides a separation of concerns between the projects, and allows both Corti and the Verhulst model to be updated independently of each other as new features are made available in both.

### **4.3.2 The Zilany Model**

The Zilany model is a very commonly used model of the auditory periphery, and robustly accounts for many phenomena observed electrophysiologically to complex stimuli. The model, originally developed based on measurements in animal models, was updated with humanized parameters to better reflect psychophysical data (Zilany et al., 2014; Zilany and Bruce, 2007, 2006).

The implementation of the Zilany model here was adapted from Rudnicki and Hemmert (2014), who provided a Python and C implementation that has been shown to produce identical output to the version documented by Zilany et al. (2014).

### **4.3.3 Variations in spontaneous rates between models**

While both the Zilany and Verhulst models produce estimates of the instantaneous firing rate of the auditory nerve, the means by which they do so are different enough that care must be taken in directly comparing their estimates.

The classification of SR types by mean spontaneous firing rate differs between the Zilany and Verhulst models. The Zilany model defines a low-SR fiber to have a spontaneous rate of 0.1 spikes/second, a medium-SR fiber to have a spontaneous rate of 10 spikes/sec, and a high-SR fiber to have a rate of 100 spikes/second. The Verhulst model defines these values as 1, 10, and 60 spikes/second, respectively. As discussed in subsection 2.3.2 and subsection 4.4.3, Temchin et al. combine low- and

medium-SR fibers into one population and define it to have a spontaneous rate of less than 18 spikes/second. For the purposes of this work, both the Zilany and Verhulst model support this approach.

#### 4.3.4 Peripheral Model Output

The Verhulst model provides estimates of response behavior at many stages of the of the auditory periphery. For models of motion in the middle ear, estimates are computed for each basilar membrane section. By default, the BM is divided into 1000 sections.

While running the simulation, the following model estimates may be stored to disk for further analysis:

1. Basilar membrane velocities for each section.
2. Basilar membrane displacements for each section.
3. Inner hair cell receptor potentials.
4. IFR for a high spontaneous rate fiber.
5. IFR for a medium spontaneous rate fiber.
6. IFR for a low spontaneous rate fiber.
7. The Otoacoustic emission.

The Zilany model, as implemented, provides IFR estimates only. Hair cell potentials could also be modeled, but are omitted.

Both models provide estimates of Instantaneous Firing Rate as a function of post-stimulus time for each combination of fiber type and best frequency, and these are passed to the next stage of the Corti environment.

## 4.4 Auditory Nerve Response Models

This stage of processing converts IFRs of specific fiber populations into an estimate of the summed activity of the auditory nerve. It corresponds to the green region of Figure 4.1.

### 4.4.1 Modeling Contributions of Inner Hair Cells

Along the Organ of Corti, each inner hair cell is innervated by multiple spiral ganglia. The Verhulst and Zilany models, however, give unitary responses for spontaneous rate type for each best center frequency, so modeling the summed response per IHC requires multiplicatively weighting and then summing the responses of each SR type to obtain the total contribution of one modeled hair cell.

Based on anatomical data (Liberman, 1978), the Verhulst model assigns 19 fibers to each inner hair cell.

The Zilany model's output is summed accordingly.

### 4.4.2 Weighting of IHC contribution

To determine which proportion of the total contribution of a given hair cell arises from fibers of a given spontaneous rate, the Verhulst model applies a scalar weighting factor to the summed Auditory Nerve Response using an undamaged nerve with 19 total fibers. Three fibers are assigned for low- and medium- SR fibers and 13 for high-SR fibers per hair cell.

Once each hair cell's contribution has been computed and summed into the total response, a scalar weighting factor was empirally chosen such that the modeled and summed response of IHCs with CFs logarithmically spaced between 175Hz and 20kHz

produces a model ABR Wave-1 amplitude of  $15 \mu\text{V}$ . For the Verhulst model, Verhulst et al. found the value of this weighting factor to be  $0.15\text{e-}6 \text{ V} \times 2.7676\text{e-}7$ .

To produce comparable results in this work, the Zilany model was scaled accordingly. By iteratively converging on a scaling factor with a tolerance of  $\pm 1 \text{ nV}$ , the scaling factor that produced an ABR Wave-1 amplitude of  $15\mu\text{V} \pm 1\text{nV}$  was found to be  $0.15\text{e-}6 \text{ V} \times 7.30282\text{e-}7$ .

#### 4.4.3 Weighting of Fiber Types per IHC

Based on data from Temchin et al. (2008), and as reviewed in section 2.3, the distribution of SR fiber types per IHC may not be uniform along the length of the basilar membrane. To account for this, we have extended the linear distribution of fiber types per hair cell with the option of a logistic distribution as a parameter.

The empirical logistic fit equation that estimates  $p$ , the percentage of fibers with spontaneous rates below 18 spikes/sec innervating a given inner hair cell as a function of best frequency was found to be:

$$p(cf) = 21 + \frac{k}{1 + e^{-r \cdot (cf - cf_0)}} \quad (4.1)$$

where  $k = 22$ ,  $r = 9\text{e-}6$  and  $cf_0 = 2500$ .

#### Fractional weights

A consequence of the approach taken in subsection 4.4.3 is that while the total fiber count per IHC is fixed at 19 fibers, the percentage of the summed response of that IHC that arises from a given fiber type is no longer guaranteed to represent an integer number of fibers. For example, a CF of 8 kHz has 42.9 percent of its innervating spiral

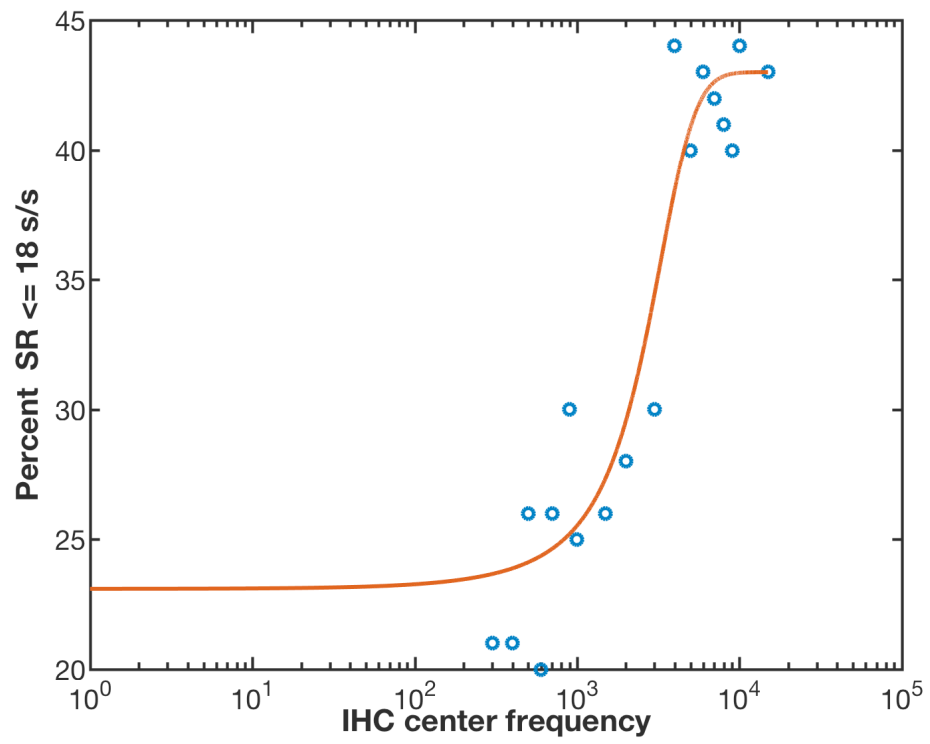


**Figure 4.2:** Experimental results (blue circles) reported by Temchin et al. were fit to a logistic model (red solid line).

ganglia with spontaneous rates below 18 spikes/second, or a total of 8.133 low and medium spontaneous rate fibers.

Therefore, it is appropriate to think of such values as weighted contributions rather than individual spiral ganglia. In the context of producing auditory nerve responses—as are used in this work—this can be thought of as providing a more accurate representation of *summed* physiological responses. Model responses of unitary fibers of different spontaneous rates are saved in the peripheral output, if desired.

#### 4.4.4 Modeling Synaptopathy

Cochlear synaptopathy is the loss of the synapse between an inner hair cell and an individual spiral ganglion. At the level of the summed auditory nerve response, selective degradation is modeled by reducing the contribution of each fiber type per hair cell by a scaling factor.

Six predetermined severity levels were chosen to model cochlear synaptopathy, all of which work in a similar manner. In each case, the portion of the response from a hair cell of a given center frequency is scaled by a percentage of its magnitude before being summed into the auditory nerve response.

### 4.5 Brainstem Models

This section details the two brainstem models in use, given by Nelson and Carney (2004) and Carney et al. (2015).

		Percentage Degradation		
Synaptopathy Type		lowSR	medSR	highSR
	none	0	0	0
	mild	10	10	10
	moderate	25	25	25
	severe	50	50	50
	ls-mild	10	10	0
	ls-moderate	25	25	0
	ls-severe	50	50	0

**Figure 4.3:** The default types of cochlear synaptopathy that may be simulated.

#### 4.5.1 The Nelson Carney 2004 Brainstem

#### 4.5.2 The Carney 2015 Brainstem

#### Choice of Best Modulation Frequency

Refer to laurel’s EPL talk spring 2016 – 100 Hz because it’s physiologically relevant. No “MTF Bank” because the science isn’t there yet. Unclear how or why they’d affect wave V delays.

### 4.6 Stimulus Generation

Corti supports simulations of stimuli of arbitrary duration and level. Simple stimuli such as clicks are generated programmatically by specifying a series of parameters such as onset time and duration, and more complex stimuli can be specified as WAV files. All WAV stimuli must specify a sound level in dB SPL re  $20\mu\text{Pa}$ ; the waveform

is then normalized by the peak value (in the case of a click) or the RMS value (for spectrally complex stimuli) and rescaled to have units of Pascals prior to simulation.

## 4.7 Automated Parameter Exploration

Corti may be run in one of two modes. In the first, a single set of parameters defines a single trajectory and the model is run once. However, while this mode of operation is convenient for fast simulations whose parameters can be defined *a priori*, it rapidly becomes impractical for situations where the relative effects of different parameter choices are to be compared, and reliable book-keeping of which parameters were used to generate which results becomes unnecessarily challenging.

Therefore, a second means of use was created, as detailed in Figure 4.4. The core of this mode is the Python Parameter Exploration Toolkit (Meyer and Obermayer, 2016). It provides the tools to allow a convenient interface to explore the parameter space generated by the specification of many available models, impairments, and options in a manner that allows easy *post-hoc* analysis. Individual trajectories may be computed in parallel on a single workstation or in a high-performance cluster so that the relative effects of each model, neuropathic impairment, and other features may be directly compared. The results for all combinations of model components are stored in one Hierarchical Data Format (HDF5) file. Comparisons of the effect of using different trajectories to the same stimuli can then be made in a way that guarantees an internally consistent analysis.

### 4.7.1 Design of new experiments

While Chapter 5 focuses on a particular combination of trajectories, designed to replicate and explore the contributions of different modeling considerations to a particular



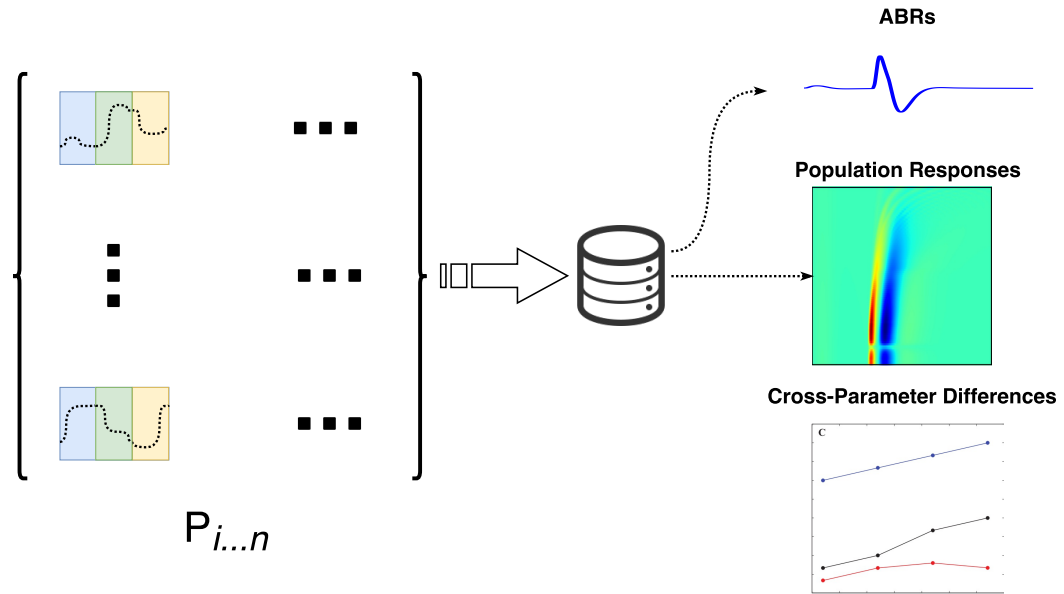


**Figure 4.4: Automated exploration of model parameters**  $P_i$  is the set of parameters required to specify one trajectory.  $N$  trajectories, where  $N$  is the cartesian product of the specified value ranges that a given parameter may take, are computed in parallel and stored in a database for further analysis.

stimulus, the method presented in section 4.7 is much more generally applicable. A modeller, using Corti, can easily design and run many other modeling experiments using these techniques for a wide variety of stimuli or parameter values.

DRAFT

## Chapter 5

# Results

### 5.1 Chapter Summary

This chapter describes the results obtained when using the modeling environment described in Chapter 4 to simulate a series of tone-in-noise experiments performed in humans by Mehraei et al. to elucidate certain aspects of cochlear synaptopathy.

### 5.2 Tone in noise

- Ran the same stimuli used by Mehraei (2015): 80dB click, varying SNR
- Ran 1208 model configurations which varied the stimulus SNR, the level and type of synaptopathy applied to the results, which peripheral model was used, whether the BM had any cf-weighting, and which brainstem model was used.
- used a python library and cluster resources to make sure the results are easily searchable.
- roughly 400 GB of model results.
- Can now examine the effects of individual parameter changes.
- can now compare results to both prior modeling results and human data.

### **5.3 Effect of peripheral model**

The verhulst and zilany models will produce different estimates of the auditory nerve response. Prior work had their results very different; with recent changes to the verhulst model, this may have changed.

### **5.4 Effect of Synaptopathy**

Six kinds of synaptopathy were simulated: uniform and low- and medium-SR specific losses of 10, 25, and 50 percent of each fiber type.

### **5.5 Effect of CF weighting**

In models of the periphery that include more low SR fibers at high frequencies, synaptopathic losses will change.

### **5.6 Effect of brainstem model**

Does our intuition about a more physiologically relevant brainstem and midbrain model capturing more of the diversity of human responses bear out?

## Chapter 6

# Discussion

### 6.1 Chapter Summary

This chapter compares the results obtained in this thesis with the human results obtained by Mehraei et al., and offers justifications and possible explanations for their similarities and differences.

### 6.2 Verhulst Model developments

### 6.3 Consequences of percentage weighting degradation for synaptopathy

## Chapter 7

## Conclusion

### 7.1 Chapter Summary

DRAFT

## References

- Bharadwaj, H. M., Masud, S., Mehraei, G., Verhulst, S., and Shinn-Cunningham, B. G. (2015). Individual differences reveal correlates of hidden hearing deficits. 35(5):2161–2172.
- Bharadwaj, H. M., Verhulst, S., Shaheen, L., Liberman, M. C., and Shinn-Cunningham, B. G. (2014). Cochlear neuropathy and the coding of supra-threshold sound. 8:26.
- Carney, L. H., Li, T., and McDonough, J. M. (2015). Speech coding in the brain: Representation of vowel formants by midbrain neurons tuned to sound fluctuations. 2(4):1–12.
- Fernandez, K. a., Jeffers, P. W. C., Lall, K., Liberman, M. C., and Kujawa, S. G. (2015). Aging after noise exposure: Acceleration of cochlear synaptopathy in “recovered” ears. 35(19):7509–7520.
- Furman, A. C., Kujawa, S. G., and Liberman, M. C. (2013). Noise-induced cochlear neuropathy is selective for fibers with low spontaneous rates. 110(3):577–86.
- Kujawa, S. G. and Liberman, M. C. (2009). Adding insult to injury: cochlear nerve degeneration after “temporary” noise-induced hearing loss. 29(45):14077–85.
- Liberman, M. C. (1978). Auditory-nerve response from cats raised in a low-noise chamber. 63(2):442–55.
- Mehraei, G. (2015). *Auditory brainstem response latency in noise as a marker of cochlear synaptopathy*. PhD thesis, Massachusetts Institute of Technology.
- Mehraei, G., Gallardo, A. P., Epp, B., Shinn-Cunningham, B., and Dau, T. (2015). Individual differences in auditory brainstem response wave-v latency in forward masking: A measure of auditory neuropathy? 137(4):2207–2207.
- Mehraei, G., Hickox, A. E., Bharadwaj, H. M., Goldberg, H., Verhulst, S., Liberman, M. C., and Shinn-Cunningham, B. G. (2016). Auditory brainstem response latency in noise as a marker of cochlear synaptopathy. 36(13):3755–3764.
- Meyer, R. and Obermayer, K. (2016). pypet: The python parameter exploration toolkit.
- Nelson, P. C. and Carney, L. H. (2004). A phenomenological model of peripheral and central neural responses to amplitude-modulated tones. 116(4):2173.

- Rudnicki, M. and Hemmert, W. (2014). Cochlea: inner ear models in python.
- Ryugo, D. (2008). Projections of low spontaneous rate, high threshold auditory nerve fibers to the small cell cap of the cochlear nucleus in cats. 154(1):114–126.
- Sergeyenko, Y., Lall, K., Liberman, M. C., and Kujawa, S. G. (2013). Age-related cochlear synaptopathy: An early-onset contributor to auditory functional decline. 33(34):13686–13694.
- Temchin, A. N., Rich, N. C., and Ruggero, M. a. (2008). Threshold tuning curves of chinchilla auditory nerve fibers. ii. dependence on spontaneous activity and relation to cochlear nonlinearity. 100(5):2899–2906.
- Verhulst, S., Bharadwaj, H. M., Mehraei, G., Shera, C. A., and Shinn-Cunningham, B. G. (2015). Functional modeling of the human auditory brainstem response to broadband stimulations. 138(3):1637–1659.
- Voysey, G. E. (2016). Corti.
- Zilany, M. S. a. and Bruce, I. C. (2006). Modeling auditory-nerve responses for high sound pressure levels in the normal and impaired auditory periphery. 120(3):1446.
- Zilany, M. S. A. and Bruce, I. C. (2007). Predictions of speech intelligibility with a model of the normal and impaired auditory-periphery. In *IEEE*, pages 481–485. IEEE.
- Zilany, M. S. A., Bruce, I. C., and Carney, L. H. (2014). Updated parameters and expanded simulation options for a model of the auditory periphery. 135(1):283–286.